A novel gait quality measure for characterizing pathological gait based on Hidden Markov Models

Abdelghani Halimi [a], Lorenzo Hermez [a], Nesma Houmani [a,*], Sonia Garcia-Salicetti [a], Omar Galarraga [b]

[a] SAMOVAR, Télécom SudParis, Institut Polytechnique de Paris, 91120 Palaiseau, France
[b] Movement Analysis Laboratory, UGECAM Ile-de-France, 77170, Coubert, France

ARTICLE INFO

ABSTRACT

This study addresses the characterization of normal gait and pathological deviations caused by neurological diseases. We focus on the angular knee kinematics in the sagittal plane and we propose to exploit Hidden Markov Models to build a statistical model of normal gait. Such model provides a log-likelihood score that quantifies gait quality. Hence allowing to assess deviations of pathological cycles from normal gait. Our approach allows a refined characterization of motor impairments of three different patients' groups. In particular, it detects the affected lower limb in Hemiparetic patients. Comparatively to the Gait Variable Score and a Dynamic Time Warping-based metric, our results show that our statistical method is more effective for finely quantifying pathological deviations. Finally, we show the potential use of our methodology to assess therapeutic impacts during gait rehabilitation, which represents a promising avenue for improving patient care.

1. Introduction

Gait, as a gross motor function, is impacted by neurological diseases that lead to different sorts of motor impairments. The advent of sensor technologies like 3D motion capture [1], Inertial Measurement Units (IMUs) [2–7] and pressure sensors [8], has enabled precise characterization of gait changes related to motor impairments.

Clinical Gait Analysis takes advantage of such advancements to quantify deviations from normal gait. Indeed, various deviation measures have been proposed in the literature, such as the Gait Deviation Index (GDI) and the Gait Profile Score (GPS) [3,9–11]. These scores are of high interest for decision-aid in clinical settings, especially for patient follow-up and for evaluating therapeutic impacts during rehabilitation.

Measuring deviations in quantified gait analysis typically involves segmenting signals into cycles, cycle normalization [12–14], and referring to a normal gait reference. Such representative is usually an average of healthy normalized gait cycles [5,15]. Pathological deviations are often measured by means of the Euclidean distance [9,11,16] as in the GDI and the GPS. More recently, the literature has pointed out the limitations of the Euclidean distance for aligning gait signals that present temporal shifts [17,18]. Such works show indeed that this practice yields a loss of precision when quantifying gait deviations.

For this reason, other works exploit Dynamic Time Warping, taking advantage of its capability to perform nonlinear time-alignments [1–3, 5,8]. However, such works quantify deviations based on a deterministic approach, since they compare a given cycle to a single reference representing normal gait. This deterministic framework cannot incorporate the intrinsic variance existing in healthy gait.

Some recent works in the literature have proposed alternatives for quantifying gait deviations. In [19], the authors proposed an Abnormality Index, based on a probabilistic framework. They estimate two Probability Density Functions (PDFs), one on healthy cycles and the other on pathological ones, per point. A modified likelihood ratio from both PDFs is then calculated per point of each cycle. However, this approach does not fully model the non-stationary nature of gait signals and depends on weights established according to ratings of an expert. This limits the gradual severity assessment of the disease [20,21].

Hidden Markov Models (HMMs) are well known for their power in capturing the dynamics of gait signals and modeling the different phases of a gait cycle [22,23]. While HMMs have primarily been exploited for gait recognition and classification [24,25], the present study proposes to use HMMs to build a statistical model of normal gait. Indeed, our first hypothesis is that the intrinsic variability of normal gait can be well captured by a statistical approach based on HMMs.

Table 1

Descriptive statistics for healthy subjects and patients.

	Healthy subjects (LUX)	Healthy subjects (CRC)	Pathological patients (CRC) "Pre-T"
Number of patients	52	52	38
Female	23	34	13
Age (Mean ± Std)	37.67 ± 13.76 (years old)	22.62 ± 3.89 (years old)	46.82 ± 12.93 (years old)
Height (Mean ± Std)	1.75 ± 0.1 (m)	1.71 ± 0.09 (m)	1.70 ± 0.10 (m)
Weight (Mean ± Std)	72.87 ± 13.07 (kg)	65.28 ± 10.77 (kg)	71.06 ± 13.99 (kg)
Speed (Mean ± Std)	1.15 ± 0.15 (m/s)	1.20 ± 0.14 (m/s)	0.52 ± 0.24 (m/s)
Number of cycles	514	526	346

Our second hypothesis is that the log-likelihood given by the model on any cycle may be used as a gait quality score, able to finely quantify gait degradation induced by neurological diseases. The third hypothesis is the potential robustness of the statistical approach when confronted to data recorded under different acquisition conditions.

To the best of our knowledge, this is the first work in the literature proposing a gait quality measure based on an HMM. In this study, our main objectives are : (*i*) to evaluate the HMM log-likelihood score for assessing motor impairments in patients with hemiparesis, paraparesis and tetraparesis; (*ii*) to study the ability of the log-likelihood score for quantifying therapeutic impacts in gait rehabilitation.

Both objectives are addressed comparatively to the state-of-the-art on gait deviation scores. Additionally, we investigate the robustness of the proposed log-likelihood score by using two datasets recorded under different acquisition conditions.

The paper is structured as follows. Section 2 describes our databases and their acquisition protocol, as well as the methodology followed in this work. Results are presented in Section 3 and discussed in Section 4. Conclusions and future work are finally stated in Section 5.

2. Materials and methods

2.1. Methodology

This retrospective study analyzes spontaneous walking data from two datasets, collected in different acquisition conditions. The first one, referred to as "LUX dataset", contains only angular kinematic data from healthy subjects. It is devoted to build a normal gait model. The second dataset, referred to as "CRC dataset", contains data from healthy subjects and patients. It is used to quantify gait deviations of healthy and pathological cycles with regard to the normal gait model, thanks to the HMM likelihood score.

We evaluate the effectiveness of such score against state-of-the-art methods, namely GPS and DTW-based scores. All scores are computed only on the knee joint kinematics in the sagittal plane (flexion/extension) because of its major role in maintaining stance stability on this plane, being characteristic of normal gait [12]. Of note, in the following we refer to the GVS (Gait Variable Score) that is the knee component of the GPS [11].

For the DTW-based score, we compute the DTW distance between each cycle from the test set (CRC dataset) to a reference gait cycle, obtained by averaging all cycles in the training set (LUX dataset). For computing the GVS, we follow the same methodology but using the Euclidean distance.

We conduct the comparative analyses through a systematic approach. We start with a global analysis of score distributions across groups, followed by an individual evaluation. Gait asymmetry is then assessed by calculating the absolute difference between the mean scores of the left and right sides for each patient. Finally, we assess the proposed method's ability in evaluating therapeutic impacts during gait rehabilitation by analyzing pre- and post-treatment scores for each patient from the CRC dataset.

To evaluate the statistical significance of differences between groups, we employ the Mann–Whitney U test, with a significance threshold set at 0.05. For significant differences, we further quantify the effect size using Cliff's delta (δ) [26]. It ranges from −1 to 1, where

$\delta = 0$ indicates no difference between groups. A $\delta < 0$ means the first group tends to have smaller values, while $\delta > 0$ suggests that the first group tends to have larger values. This provides a clear measure of both the magnitude and direction of the observed differences.

2.2. Data collection and description

2.2.1. LUX dataset

This dataset contains angular kinematic signals from 52 healthy subjects with no neuro-orthopaedic trouble, for three joints (knee, ankle and hip) in the sagittal plane. Further details are given in Table 1.

Data were collected at the "Centre National de Rééducation Fonctionnelle et de Réadaptation" - Rehazenter, Luxembourg [27]. All participants gave informed written consent prior to their inclusion and the protocol was conformed to the Declaration of Helsinki and approved by the Ethics Committee of the Rehazenter. This dataset is available online for academic and research purposes [27].

The 3D trajectories of 24 reflective skin markers were recorded using the 10-camera optoelectronic system (OQUS-4, Qualisys AB, Sweden) sampled at 100 Hz. All data were processed with a custom Matlab program based on the Biomechanical ToolKit (BTK). The joint kinematics were calculated using the 3D Kinematics and Inverse Dynamics toolkit proposed by Dumas, and freely available on the MathWorks File Exchange [27].

Participants were asked to walk on a straight 10-m walkway under five walking speed conditions. In this study, we only exploit the data recorded at spontaneous walking speed. The available walking sequences (cycles) were normalized as a percentage of the total duration of the walking cycle over 101 points.

2.2.2. CRC dataset

We exploit angular kinematic data acquired during a spontaneous walking task from 52 healthy subjects and 38 patients suffering from neurological diseases, such as cerebral palsy, traumatic brain injury, spinal cord injury, stroke or multiple sclerosis. Table 1 reports more details.

Data was collected at the "Centre de Réadaptation de Coubert" of UGECAM Ile-de-France, which is a healthcare institution specialized in neuromotor rehabilitation. Each participant was informed that his/her data might be used for research purposes, and no participant objected to the use of his/her data. This retrospective study was approved on April 10th, 2019 by the internal Ethics Committee of UGECAM Ile-de-France.

Data acquisition was carried out using the Codamotion optoelectronic system, integrating four CX1 cameras placed in each corner of the laboratory. The system recovers angle kinematics during walking for five joints (pelvis, hip, foot, ankle and knee) in three planes (sagittal, frontal and transverse), with a sampling rate of 100 Hz. People were asked to walk naturally for 10 m in a straight line on flat ground, at a spontaneous speed. This process was repeated five times in average, each time corresponding to a trial. The angular kinematics of each joint, captured during each gait trial, is a periodic signal consisting of different consecutive cycles, defined between the initial contact event and the terminal swing event. This complete signal was segmented into gait cycles, automatically detected with the high-pass algorithm [28]

Table 2

Descriptive statistics for pathological subjects of the CRC dataset.

	Hemiparesis (HP)	Paraparesis (PP)	Tetraparesis (TP)
Number of patients	18	9	11
Female	6	4	3
Age (Mean ± Std)	47.78 ± 13.85 (years old)	48.44 ± 8.37 (years old)	43.90 ± 14.94 (years old)
Height (Mean ± Std)	1.72 ± 0.11 (m)	1.65 ± 0.10 (m)	1.71 ± 0.09 (m)
Weight (Mean ± Std)	74.53 ± 12.90 (kg)	64.30 ± 13.06 (kg)	70.90 ± 15.55 (kg)
Speed (Mean ± Std)	0.45 ± 0.23 (m/s)	0.62 ± 0.28 (m/s)	0.55 ± 0.18 (m/s)
Number of cycles	162	78	106

Table 3

Descriptive statistics for the training and validation sets.

	Train set	Validation set
Number of cycles	384	130
Age (Mean ± Std)	37,69 ± 13.57	37.62 ± 14.37
Number of persons	39	13

and controlled by an expert. The gait cycles were normalized into 51 points (*i.e.*, 1 point for every 2% of the gait cycle).

The healthy subjects recruited did not suffer from any disease affecting motor function. Patients show different motor deficiencies affecting one lower limb as in patients with hemiparesis (HP), or both lower limbs as in patients with paraparesis (PP) or tetraparesis (TP) (also affecting upper limbs). The dataset contains 18 patients with HP, 9 patients with PP and 11 patients with incomplete TP. The characteristics of patients per motor impairment are given in Table 2.

2.3. Data preprocessing and partitioning

As gait cycles from both datasets do not have the same lengths, we normalize the cycles from LUX dataset into 51 points, by selecting one point out of two. Additionally, we apply a Z-score transformation to them on a cycle-by-cycle basis to exploit simultaneously both datasets.

In the following, we use LUX dataset for both training and validation purposes, in particular because it exhibits the broadest age distribution of the healthy population (see Table 1). As depicted in Table 3, 75% and 25% of cycles belong respectively to the training and validation sets, ensuring a similar age distribution in both sets. Also, we impose that cycles belonging to a same individual cannot be included in both sets; in other words, each person's cycles are exclusive to one set. Finally, CRC dataset serves as our test set for gait quality assessment.

2.4. Proposed HMM-based approach

The Hidden Markov Model (HMM) is a double stochastic process [29] with hidden states that are not directly observable but can be inferred through observable stochastic processes. The model structure includes states, transition probabilities, and a set of probability distributions that can be either discrete or continuous, depending on the type of observations $O = (O_t)$, where O_t is the observation at time t.

Let us denote by $S = \{s_1, s_2, s_3, \ldots, s_N\}$ the state vector, where N represents the number of states in the model and the state s_i visited at time t is denoted by the variable q_t.

The complete parameter set in the case of a continuous HMM is often defined in the literature such as $\lambda = (A, B, \pi)$, where:

- $A = \{a_{ij}\}$ is the transition probability distribution matrix, where:

$$a_{ij} = P\left(s_j = q_{t+1} \mid s_i = q_t\right), 1 \leq i, j \leq N \tag{1}$$

- The emission law of observation O_t by each state j is modeled using a multivariate Gaussian mixture, such as:

$$b_j(O_t) = \sum_{m=1}^{M} c_{jm} \mathcal{N}\left(O_t; \mu_{jm}, \Sigma_{jm}\right), \tag{2}$$
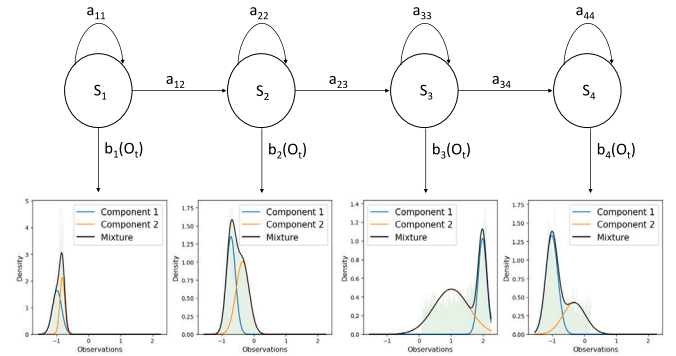

Fig. 1. A four-state, left-to-right HMM. Each state is modeled using a mixture density (depicted in black) of two diagonal Gaussians.

where M is the number of Gaussian mixtures per state, c_{jm} is the mixture coefficient for the mth mixture in state j, $\mathcal{N}\left(O_t; \mu_{jm}, \Sigma_{jm}\right)$ represents the multivariate Gaussian density of mean vector μ_{jm} for the mth mixture in state j and Σ_{jm} is the corresponding covariance matrix.

- The initial probability distribution is denoted by $\pi = \{\pi_i\}$, where:

$$\pi_i = P\left(s_i = q_1\right), 1 \leq i \leq N \tag{3}$$

In this study, we propose to train a continuous HMM on normalized gait cycles of healthy subjects from LUX dataset (refer to Table 3). Then, we compute the log-likelihood score for each cycle in the test set (CRC dataset), and consider this score as our gait quality metric.

Consistent with the existing literature [30–32], we chose to model gait cycles using a four-state left-to-right topology (see Fig. 1), where each state corresponds to a gait phase. This topology is well suited to model normal gait due to the sequential evolution of gait phases.

As the number of states is equal to four, the only hyper-parameter to tune is the number of mixtures M. This number reflects a trade-off between the complexity of the model and its performance. We trained the HMM using the Baum-Welch algorithm (also known as the Expectation–Maximization algorithm) [29]. This algorithm estimates the parameters of the HMM to optimize the likelihood of the observed sequence on the training set. The training process stops when the model converges, with a set tolerance of 10^{-3}. For the inference phase, the model employs the Viterbi algorithm to decode the state sequence based on each provided observation (a gait cycle) [29]. In this study, we use in each state a mixture of two diagonal Gaussians, as this configuration yielded the highest likelihood score on the validation set. The obtained Gaussian densities for the four states are displayed in Fig. 1.

3. Experimental results

In this section, we present the results obtained using HMM likelihood scores comparatively to GVS and DTW methods. To facilitate comparisons, we normalize the scores for each method to a range of 0 to 1 using the min–max scaler. Of note, HMM score is inversely
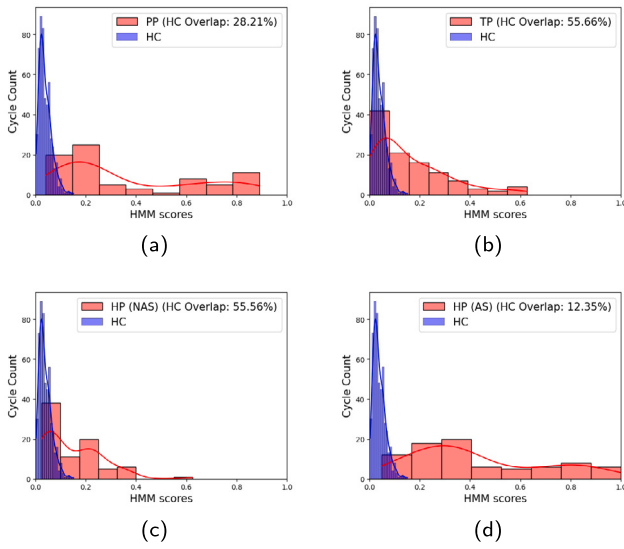
Fig. 2. Histograms and kernel density curves of normalized HMM scores for HC (in blue) and patients (in red) with: (a) PP, (b) TP, (c) HP considering only their Non-Affected Side, and (d) HP considering only their Affected Side.
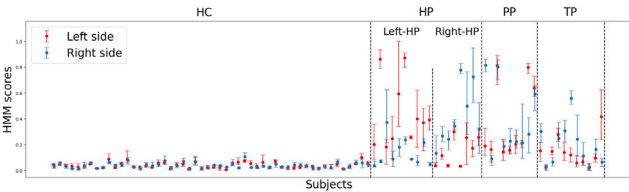

Fig. 3. Distribution of normalized HMM scores in bar plots for HC and patients with HP, PP and TP, considering the left side (in red) and the right side (in blue) separately.

normalized to maintain consistency across methods. Therefore, for all scores, a zero value denotes a gait quality resembling normal gait, and a higher value indicates a deterioration in gait.

3.1. Results of the HMM-based approach

Fig. 2 displays the normalized HMM likelihood scores on the CRC dataset, for Healthy Controls (HC) and patients with HP, PP, TP, by separating the Affected Side (AS) from the Non-Affected Side (NAS) for HP.

Fig. 2 first reveals low HMM scores for HC and high values for patients, as expected. We also observe a sharp distribution for HC scores, whereas those of patients show an important variance. This suggests that this method is well-suited for normal gait characterization. Besides, TP and HP-NAS groups exhibit the highest percentage of overlap with HC (55.66% and 55.56% respectively). On the other hand, PP and HP-AS groups show the lowest percentage of overlap with HC (28.21% and 12.35% respectively). These results are consistent with the nature of gait impairment associated to each group of patients.

Fig. 3 displays the distribution of HMM scores per person considering, separately, the left side of the body (in red) and the right side (in blue). Each side of the body is represented per person by a bar plot illustrating the mean HMM score computed on all cycles for that side, as well as the upper and lower bounds representing the complete range of scores. For a clearer visualization, HC are grouped to the left, while patients are categorized by motor impairment to the right in the following order: HP with Left affected side (Left-HP), HP with the Right affected side (Right-HP), PP and then TP.

We observe again in Fig. 3 that HMM scores for HC exhibit very low score values and low variance compared to patients. Regarding
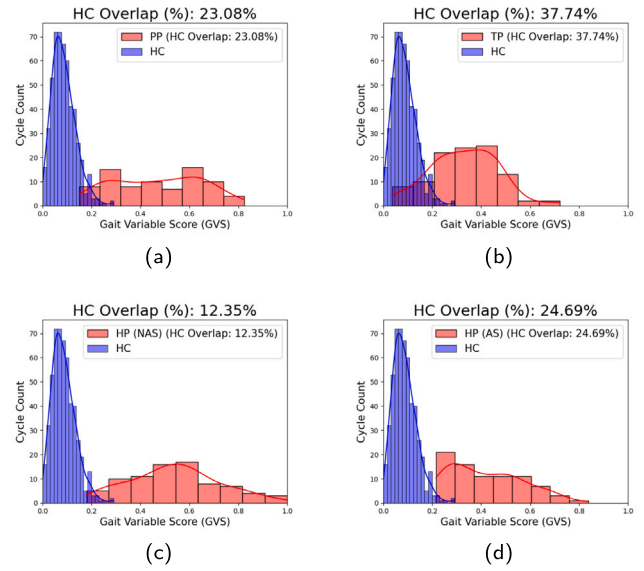

Fig. 4. Histograms and kernel density curves of normalized GVS scores for HC (in blue) and patients (in red) with: (a) PP, (b) TP, (c) HP considering only their Non-Affected Side, and (d) HP considering only their Affected Side.

HP, we note that the affected side exhibits consistently higher score values than the non-affected side, except for one left-HP. Moreover, the affected side in HP patients shows higher score variance comparatively to the corresponding non-affected side. This result reflects the tendency of the affected side in producing more gait variability. Additionally, we note that for some HP patients, their non-affected side exhibits the same behavior as HC in terms of score values and variance.

Finally, we observe an increasing trend of the HMM scores when moving from incomplete TP to PP and from PP to HP. This trend is consistent with the fact that TP group in the CRC dataset consists mostly of incomplete cases of TP, while the HP and PP groups represent cases of greater impairment.

3.2. Comparison to GVS and DTW methods

Figs. 4 and 5 represent the distributions of GVS and DTW scores, respectively, for HC and patients.

As with the normalized HMM score, we note that the normalized GVS and DTW scores show low values for HC, contrary to patients. However, the distribution of GVS scores for HC is more spread than those of HMM and DTW scores.

Regarding the percentage of overlap between the score distribution of HC and HP, we observe a high overlap between HC and HP-NAS, and a low overlap between HC and HP-AS in terms of DTW scores, as with HMM. By contrast, this trend is inverted with the GVS score, as indicated in Fig. 4: HP-AS group shows 24.69% of overlap with HC, whereas HP-NAS group shows 12.35% of overlap with HC. These first results suggest a better characterization of normal gait and of patients' motor impairments with HMM and DTW.

For a deeper analysis, we plot in Fig. 6 the distribution of normalized GVS and DTW scores per person considering, separately, the left side of the body (in red) and the right side (in blue).

Interestingly, based on the GVS score, we observe in HP patients that the impacted side does not always have the highest score. Besides, there is no clear differentiation between the affected and non affected sides. With DTW and HMM, the opposite trend is observed. Indeed, with the latter methods, the impacted side displays greater values and variance than the non-affected one (see Fig. 6b and Fig. 3). However, the distinction between the affected and non affected sides remains less pronounced with DTW comparatively to HMM.
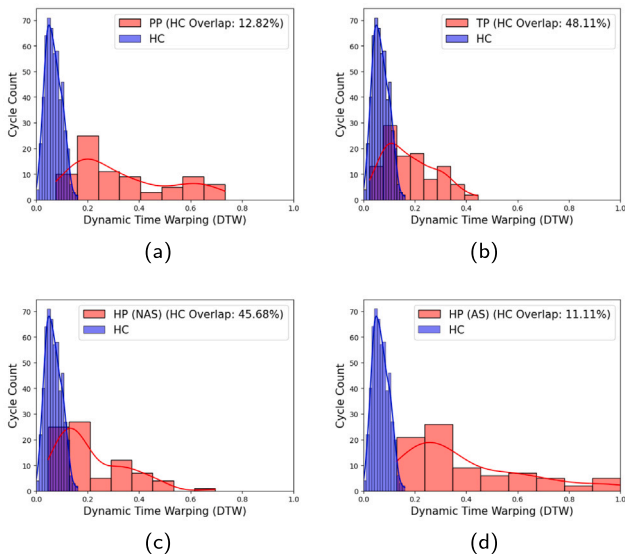
Fig. 5. Histograms and kernel density curves of normalized DTW scores for HC (in blue) and patients (in red) with: (a) PP, (b) TP, (c) HP considering only their Non-Affected Side, and (d) HP considering only their Affected Side.
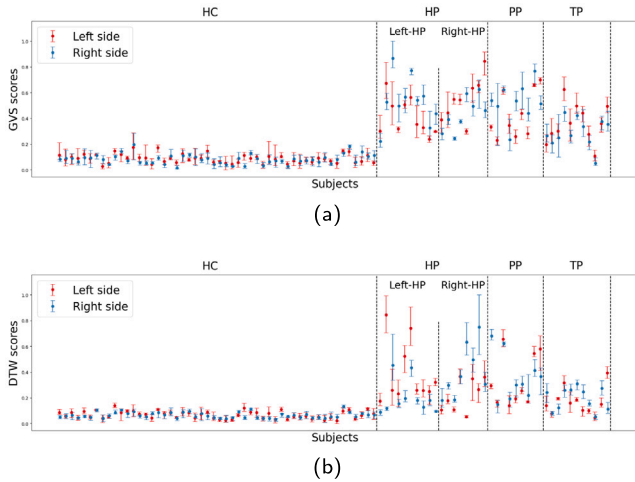

Fig. 6. Distribution of normalized scores in bar plots for HC and patients with HP, PP and TP, considering the left side (in red) and the right side (in blue) separately using: (a) GVS and (b) DTW.

Using the Mann–Whitney test, all methods show statistically significant differences between groups (p-value < 0.05), except between HP and PP for all methods. In addition, the difference between the affected and the non-affected sides in HP is more significant with HMM ($\delta = 0.72$) and DTW ($\delta = 0.54$) comparatively to GVS ($\delta = -0.38$). Moreover, the negative value of the Cliff's delta value obtained on GVS reflects the inversion trend between HP-AS and HP-NAS.

These findings point out the weakness of GVS in finely quantifying the degree of motor impairments, especially when exploiting angular kinematic data acquired in different acquisition conditions.

In the following, for a deeper analysis, we go a step forward by assessing the potential of HMM and DTW scores for gait symmetry measurement.

3.3. Gait asymmetry analysis

Based on the previous results, we study gait asymmetry using only normalized HMM and DTW scores, by calculating the absolute difference between the mean scores of the left and right sides of the body.
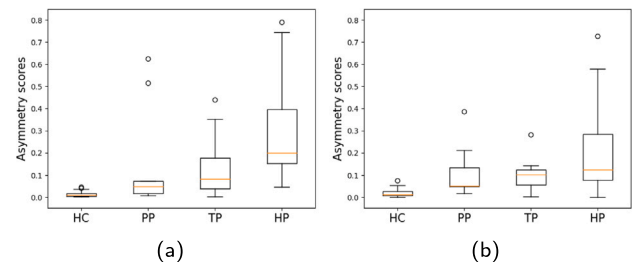

Fig. 7. Boxplots of asymmetry scores associated with HC and patients with HP, PP and TP using: (a) HMM and (b) DTW scores.

A smaller asymmetry score implies a more symmetrical gait, whereas a higher score could suggest potential gait abnormalities, which may be indicative of a pathological condition or injury. Fig. 7 shows the distribution of asymmetry scores for HC and patients using HMM and DTW-based methods.

HC show the lowest asymmetry scores with both HMM and DTW methods, reflecting the natural symmetry of healthy gait (see Fig. 7). Besides, HP are those presenting the highest asymmetry scores with both measures, reflecting the unilateral impact of the pathology. In between these two extreme behaviors, we observe a progressive trend of HMM asymmetry scores, which increases when moving from HC to PP, TP and then to HP. For the PP group, the asymmetry scores are generally lower than those of HP because of the bilateral impact of the pathology in this population. For the TP group, asymmetry scores are more variable: as shown in Fig. 3, for some TP patients there is a stronger degradation on one side of the body, whereas for some other TP patients, both sides are affected.

This progressive trend from HC to HP is not observed with DTW asymmetry scores (see Fig. 7b). Indeed, although the HC and HP groups remain exhibiting the two extreme behaviors, there is no longer a differentiation between PP and TP.

These observations are in line with the statistical analysis that reveals that the HMM shows significant differences between all groups ($p < 0.05$) except between TP and PP. Nevertheless, DTW fails to show significant differences between several groups (HP vs. TP, HP vs. PP, and TP vs. PP). Moreover, the HMM achieves a perfect separation between HC and HP with $\delta = 1$, which decreases between HC and PP ($\delta = 0.58$). In comparison, DTW achieves $\delta = 0.88$ for HC vs. HP and $\delta = 0.84$ for HC vs. PP. This highlights HMM's superior sensitivity to smaller asymmetry differences and its finer quantification of gait symmetry among patients' populations.

These results highlight the limit of the DTW-based method for characterizing the relative behavior of different patients' groups. Actually, the DTW-based methods exploits an average waveform representing normal gait, which cannot represent well enough the natural variability present in the healthy population. By contrast, our proposed HMM-based approach encompasses this variability by its statistical nature. This major advantage allows a finer characterization of deviations from normal gait, according to each patients' group. This leads to a specific characterization per patients' group and an explainable relative behavior between them.

3.4. HMM-based gait assessment in rehabilitation

We exploit the HMM score for assessing patients' evolution during a rehabilitation process. At the "Centre de Rééducation de Coubert", patients followed rehabilitation and our CRC dataset contains gait sequences from two different sessions: one before treatment and another after treatment. Both sessions were captured in the same conditions and with the same protocol previously described in Section 2.2.2. Tables 1 and 4 contain the description of patients before treatment (Pre-T) and after treatment (Post-T), respectively.
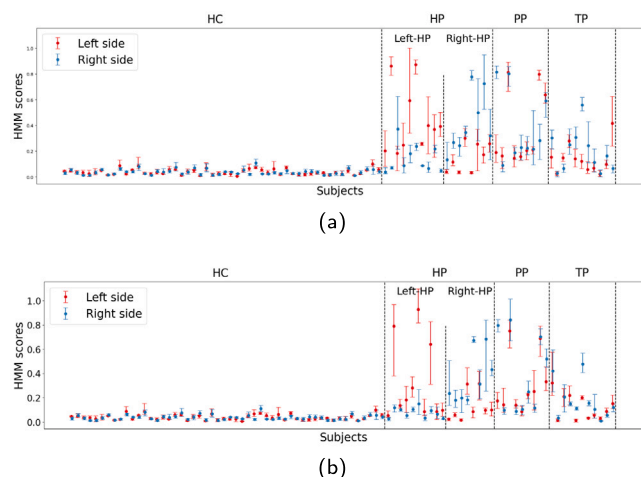
(a)

(b)

Fig. 8. Distributions of HMM-based gait quality scores for HC and patients with HP, PP, and TP at: (a) pre-treatment and (b) post-treatment.

Table 4
Descriptive statistics for CRC patients (Post-T).

	CRC Patients "Post-T"
Number of patients	38
Female	13
Age (Mean ± Std)	46.89 ± 12.98 (years old)
Height (Mean ± Std)	1.70 ± 0.10 (m)
Weight (Mean ± Std)	71.55 ± 13.55 (kg)
Number of cycles	374

Table 5
Cliff's delta values before and after treatment between HC and patients.

	HC vs. HP	HC vs. PP	HC vs. TP
Pre-treatment	0.84	0.98	0.65
Post-treatment	0.72	0.96	0.45

Fig. 8 shows the distributions of HMM scores per individual for HC as well as for patients before treatment (Fig. 8a) and after treatment (Fig. 8b).

The majority of patients exhibit a decrease in post-treatment HMM scores and a lower variance (Fig. 8b) compared to pre-treatment scores (Fig. 8a). This reveals the shift of patient's behavior after treatment towards that of the HC group. More precisely, after treatment, the Cliff's delta value between HC and patients' groups is lower than those obtained before treatment, as reported in Table 5.

Additionally, this trend is also observed when comparing the HMM scores between the affected and non-affected sides in HP patients. Indeed, after treatment, the Cliff's delta significantly decreases from 0.72 to 0.25, which reflects an improvement of gait symmetry after rehabilitation. These findings underscore the sensitivity of our HMM-based score in capturing therapeutic effects on gait quality.

4. Discussion

In this retrospective study, we exploited a novel gait quality measure based on the likelihood score derived from an HMM. To this end, we have used two datasets : one for modeling healthy gait and the other one for quantifying gait deviations for both healthy subjects and patients with different motor impairments. We compared our proposed HMM score to the traditional GVS and DTW-based scores, since we considered only the knee joint kinematics in the sagittal plane.

Results showed that DTW and HMM-based approaches both lead to a sharp HC scores distribution on the CRC dataset, proving a stronger generalization power, especially when using data acquired with different acquisition systems. However, the GVS shows a larger HC scores'

distribution and fails to distinguish between the impacted and non-impacted sides in the HP population. This was further confirmed by Cliff's delta value that revealed a lower and negative value for the GVS, in contrast to DTW and HMM, for which the distinction was more pronounced: $\delta = -0.38$ for GVS, compared to $\delta = 0.72$ for HMM and $\delta = 0.54$ for DTW. This can be explained by the fact that the GVS cannot handle local distortions and time-shifts between gait signals, unlike DTW and HMM. For these reasons, it lacks the sensitivity required to distinguish between the impacted and non-impacted sides in the HP population.

Moreover, DTW and HMM-based methods provide a refined characterization of motor impairments, thanks to their ability to capture the dynamics of gait signals. However, the HMM-based method outperforms the DTW-based approach in distinguishing the three motor impairments under study. Indeed, by computing an asymmetry score for bilateral gait, we observed a progressive increase of such score from HC to PP, TP and then HP, with HMM likelihood scores and not with DTW scores.

In addition, the statistical analysis revealed that the HMM scores lead to significant differences between all groups, except between TP and PP, whereas DTW failed to demonstrate significant differences between several groups. Moreover, the HMM achieved a higher separation between HC and HP compared to DTW. The HMM also showed a lower separation between HC and PP compared to DTW, highlighting the higher ability of the HMM for finely quantifying differences in symmetry between patients' groups.

Actually, the DTW-based method has the drawback on relying on an average waveform accounting for normal gait, which cannot represent well enough the natural variability present in the healthy population. By contrast, our proposed HMM-based approach models this variability thanks to its statistical nature. This major advantage leads to a finer characterization of deviations from normal gait depending on each patients' group.

Finally, our HMM-based approach was used to assess gait quality progress after rehabilitation. Our results showed that post-treatment cycles get closer to HC cycles' behavior. Indeed, we found that Cliff's delta between HC and the other groups in the post-treatment setting is lower than in the pre-treatment setting (0.72 vs. 0.84 for HC and HP; 0.96 vs. 0.98 for HC and PP; 0.45 vs. 0.65 for HC and TP). A similar trend was observed when comparing the scores between HP (AS) and (NAS) groups, where Cliff's delta significantly dropped from 0.72 to 0.25 post-treatment. These findings underscore the sensitivity of our proposed gait quality measure in detecting therapeutic effects.

Consequently, this work confirmed our previous findings [17,18] that DTW outperforms traditional metrics like GVS in assessing gait quality. However, we found that the HMM-based method provides a finer and a more sensitive score due to the ability of the HMM to capture subtle variations in gait cycles, thanks to its statistical nature. Thus, while DTW remains effective, the HMM offers an even more precise assessment of gait deviations, making it an accurate tool for evaluating motor impairments and rehabilitation progress.

There are two main limitations to this study. First, we conducted our experiments on two datasets of limited size. Nevertheless, such datasets were found useful to evaluate the generalization power of our approach when confronted to data acquired with different acquisition systems. One additional weakness consists in the use of time-normalized gait signals, as frequently done in the literature. Indeed, as investigated in [17], this leads to a loss of information that may contribute to a more refined characterization of individuals. Actually, the HMM is well suited for handling sequences of different lengths. This was not addressed in the current study because the LUX dataset contains only normalized angular kinematics data.

5. Conclusion

In this study, we proposed to use Hidden Markov Models (HMM) for human gait analysis at two levels : firstly, for building a normal gait model to represent gait dynamics in the healthy population; secondly, for retrieving a gait quality metric to quantify healthy and pathological gait deviations through the HMM likelihood score.

Experimental results demonstrated that the statistical modeling of gait dynamics with HMM is useful for capturing the intrinsic variability in the healthy population, and provides a fine characterization of motor impairments in terms of gait degradation and bilateral gait asymmetry. Our HMM-based approach was also found powerful for the assessment of gait quality progress after rehabilitation.

Further experiments should be conducted on larger datasets to confirm the potential of our approach for gait analysis. Furthermore, in this work we applied the HMM on time-normalized signals and considering only the knee joint kinematics. It might be interesting to consider raw signals to keep the temporal properties of gait cycles and to extend our analysis to additional joint kinematics and planes.

CRediT authorship contribution statement

Abdelghani Halimi: Writing – review & editing, Visualization, Validation, Software, Methodology, Investigation, Formal analysis, Data curation. **Lorenzo Hermez:** Writing – review & editing, Validation, Formal analysis, Data curation. **Nesma Houmani:** Writing – review & editing, Validation, Supervision, Resources, Methodology, Investigation, Formal analysis, Conceptualization. **Sonia Garcia-Salicetti:** Writing – review & editing, Validation, Supervision, Resources, Methodology, Investigation, Formal analysis, Conceptualization. **Omar Galarraga:** Validation, Data curation.

Declaration of competing interest

The authors declare no conflict of interest regarding this work and the authors.

Acknowledgment

References

[1] M. Błażkiewicz, K. Lann Vel Lace, A. Hadamus, Gait symmetry analysis based on dynamic time warping, Symmetry 13 (5) (2021) 836.

[2] X. Wang, M. Kyrarini, D. Ristić-Durrant, M. Spranger, A. Gräser, Monitoring of gait performance using dynamic time warping on IMU-sensor data, in: 2016 IEEE International Symposium on Medical Measurements and Applications (MeMeA), IEEE, 2016, pp. 1–6.

[3] X. Wang, D. Ristic-Durrant, M. Spranger, A. Gräser, Gait assessment system based on novel gait variability measures, in: 2017 International Conference on Rehabilitation Robotics, ICORR, IEEE, 2017, pp. 467–472.

[4] R. Caldas, M. Mundt, W. Potthast, F.B. de Lima Neto, B. Markert, A systematic review of gait analysis methods based on inertial sensors and adaptive algorithms, Gait Posture 57 (2017) 204–210.

[5] H. Zhao, H. Xu, Z. Wang, L. Wang, S. Qiu, D. Peng, J. Li, J. Jiang, Analysis and evaluation of hemiplegic gait based on wearable sensor network, Inf. Fusion 90 (2023) 382–391.

[6] A. Talitckii, E. Kovalenko, A. Shcherbak, A. Anikina, E. Bril, O. Zimniakova, M. Semenov, D.V. Dylov, A. Somov, Comparative study of wearable sensors, video, and handwriting to detect Parkinson's disease, IEEE Trans. Instrum. Meas. 71 (2022) 1–10.

[7] T.T. Pham, Y.S. Suh, Conditional generative adversarial network-based regression approach for walking distance estimation using waist-mounted inertial sensors, IEEE Trans. Instrum. Meas. 71 (2022) 1–13.

[8] Y.-K. Jeong, K.-R. Baek, Asymmetric gait analysis using a DTW algorithm with combined gyroscope and pressure sensor, Sensors 21 (11) (2021) 3750.

[9] V. Cimolin, M. Galli, Summary measures for clinical gait analysis: A literature review, Gait Posture 39 (4) (2014) 1005–1010.

[10] M.H. Schwartz, A. Rozumalski, The Gait Deviation Index: a new comprehensive index of gait pathology, Gait Posture 28 (3) (2008) 351–357.

[11] R. Baker, J.L. McGinley, M.H. Schwartz, S. Beynon, A. Rozumalski, H.K. Graham, O. Tirosh, The gait profile score and movement analysis profile, Gait Posture 30 (3) (2009) 265–269, http://dx.doi.org/10.1016/j.gaitpost.2009.05.020, URL https://www.sciencedirect.com/science/article/pii/S0966636209001489.

[12] A. Bonnefoy-Mazure, S. Armand, Normal gait, Orthop. Manag. Child. with Cereb. Palsy Ed. by Federico Canavese Jacques Deslandes 40, 2015, 645–657.

[13] M. Burnfield, Gait analysis: normal and pathological function, J. Sports Sci. Med. 9 (2) (2010) 353.

[14] D.A. Winter, Biomechanics and motor control of human gait: normal, elderly and pathological, 1991.

[15] T. Lencioni, I. Carpinella, M. Rabuffetti, A. Marzegan, M. Ferrarin, Human kinematic, kinetic and EMG data during different walking and stair ascending and descending tasks, Sci. Data 6 (1) (2019) 309.

[16] D.S. Speciali, E.M. Oliveira, J.R. Cardoso, J.C.F. Correa, R. Baker, P.R.G. Lucareli, Gait profile score and movement analysis profile in patients with parkinson's disease during concurrent cognitive load, Braz. J. Phys. Ther. 18 (4) (2014) 315–322, http://dx.doi.org/10.1590/bjpt-rbf.2014.0049.

[17] L. Hermez, A. Halimi, N. Houmani, S. Garcia-Salicetti, O. Galarraga, V. Vigneron, Clinical gait analysis: Characterizing normal gait and pathological deviations due to neurological diseases, Sensors 23 (14) (2023) http://dx.doi.org/10.3390/s23146566, URL https://www.mdpi.com/1424-8220/23/14/6566.

[18] L. Hermez, N. Houmani, S. Garcia-Salicetti, O. Galarraga, V. Vigneron, Gait deviation and neurological diseases: A comparative study of quantitative measures, in: 11th IEEE International Conference on E-Health and Bioengineering (EHB 2023), 2023.

[19] R. Bajpai, D. Joshi, A-GAS: A probabilistic approach for generating automated gait assessment score for cerebral palsy children, IEEE Trans. Neural Syst. Rehabil. Eng. 29 (2021) 2530–2539.

[20] L. Tang, X. Wang, P. Lian, Z. Lu, Q. Zheng, X. Yang, Q. Hu, H. Zheng, Wearable sensor-based multi-modal fusion network for automated gait dysfunction assessment in children with cerebral palsy, Adv. Intell. Syst. (2024) 2300845.

[21] C. Yoon, Y. Jeon, H. Choi, S.-S. Kwon, J. Ahn, Interpretable classification for multivariate gait analysis of cerebral palsy, BioMed. Eng. OnLine 22 (1) (2023) 109.

[22] N. Roth, A. Küderle, M. Ullrich, T. Gladow, F. Marxreiter, J. Klucken, B. Eskofier, F. Kluge, Hidden Markov model based stride segmentation on unsupervised free-living gait data in Parkinson's disease patients, J. Neuroeng. Rehabil. 18 (1) (2021) 93, http://dx.doi.org/10.1186/s12984-021-00883-7.

[23] J. Taborri, S. Rossi, E. Palermo, F. Patanè, P. Cappa, A novel HMM distributed classifier for the detection of Gait phases by means of a wearable inertial sensor network, Sensors 14 (9) (2014) 16212–16234, http://dx.doi.org/10.3390/s140916212, URL https://www.mdpi.com/1424-8220/14/9/16212.

[24] H.-I. Suk, B.-K. Sin, HMM-based Gait recognition with human profiles, in: D.-Y. Yeung, J.T. Kwok, A. Fred, F. Roli, D. de Ridder (Eds.), Structural, Syntactic, and Statistical Pattern Recognition, Springer Berlin Heidelberg, Berlin, Heidelberg, 2006, pp. 596–603.

[25] K. Iwamoto, K. Sonobe, N. Komatsu, A gait recognition method using HMM, in: SICE 2003 Annual Conference (IEEE Cat. No.03TH8734), Vol. 2, 2003, pp. 1936–1941.

[26] N. Cliff, Dominance statistics: Ordinal analyses to answer ordinal questions, Psychol. Bull. 114 (3) (1993) 494.

[27] F. Moissenet, F. Leboeuf, S. Armand, Lower limb sagittal gait kinematics can be predicted based on walking speed, gender, age and BMI, Sci. Rep. 9 (1) (2019) 9510, http://dx.doi.org/10.1038/s41598-019-45397-4.

[28] E. Desailly, Y. Daniel, P. Sardain, P. Lacouture, Foot contact event detection using kinematic data in cerebral palsy children and normal adults gait, Gait Posture 29 (1) (2009) 76–80.

[29] L. Rabiner, A tutorial on hidden Markov models and selected applications in speech recognition, Proc. IEEE 77 (2) (1989) 257–286, http://dx.doi.org/10.1109/5.18626.

[30] M. Sánchez-Manchola, L. Arciniegas-Mayag, M. Múnera, M. Bourgain, T. Provot, C.A. Cifuentes, Effects of stance control via hidden Markov model-based gait phase detection on healthy users of an active hip-knee exoskeleton, Front. Bioeng. Biotechnol. 11 (2023) http://dx.doi.org/10.3389/fbioe.2023.1021525, URL https://www.frontiersin.org/articles/10.3389/fbioe.2023.1021525.

[31] L. Liu, H. Wang, H. Li, J. Liu, S. Qiu, H. Zhao, X. Guo, Ambulatory human gait phase detection using wearable inertial sensors and hidden Markov model, Sensors 21 (4) (2021) http://dx.doi.org/10.3390/s21041347, URL https://www.mdpi.com/1424-8220/21/4/1347.

[32] A. Mannini, A.M. Sabatini, A hidden Markov model-based technique for gait segmentation using a foot-mounted gyroscope, in: 2011 Annual International Conference of the IEEE Engineering in Medicine and Biology Society, 2011, pp. 4369–4373, http://dx.doi.org/10.1109/IEMBS.2011.6091084.